Leonardo da Vinci's illustration of the swirling flow of turbulence.
(*The Royal Collection © 2004, Her Majesty Queen Elizabeth II*)

The Turbulence Problem

An Experimentalist's Perspective

Robert Ecke

Turbulent fluid flow is a complex, nonlinear multiscale phenomenon, which poses some of the most difficult and fundamental problems in classical physics. It is also of tremendous practical importance in making predictions—for example, about heat transfer in nuclear reactors, drag in oil pipelines, the weather, and the circulation of the atmosphere and the oceans. But what is turbulence? Why is it so difficult to understand, to model, or even to approximate with confidence? And what kinds of solutions can we expect to obtain? This brief survey starts with a short history and then introduces both the modern search for universal statistical properties and the new engineering models for computing turbulent flows. It highlights the application of modern supercomputers in simulating the multiscale velocity field of turbulence and the use of computerized data acquisition systems to follow the trajectories of individual fluid parcels in a turbulent flow. Finally, it suggests that these tools, combined with a resurgence in theoretical research, may lead to a "solution" of the turbulence problem.

Many generations of scientists have struggled valiantly to understand both the physical essence and the mathematical structure of turbulent fluid motion (McComb 1990, Frisch 1995, Lesieur 1997). Leonardo da Vinci (refer to Richter 1970), who in 1507 named the phenomenon he observed in swirling flow "la turbolenza" (see the drawing on the opening page), described the following picture: "Observe the motion of the surface of the water, which resembles that of hair, which has two motions, of which one is caused by the weight of the hair, the other by the direction of the curls; thus the water has eddying motions, one part of which is due to the principal current, the other to the random and reverse motion."

Two aspects of da Vinci's observations remain with us today. First, his separation of the flow into a mean and a fluctuating part anticipates by almost 400 years the approach taken by Osborne Reynolds (1894). The "Reynolds decomposition" of the fluid velocity into mean and fluctuating parts underpins many engineering models of turbulence in use today.[1] Second, da Vinci's identification of "eddies" as intrinsic elements in turbulent motion has a modern counterpart: Scientists today are actively investigating the role of such structures as the possible "sinews" of turbulent dynamics.

Long after da Vinci's insightful observations, a major step in the description of fluid flows was the development of the basic dynamical equation of fluid motion. The Euler equation of motion (written down in the 18th century) describes the conservation of momentum for a fluid without viscosity, whereas the Navier-Stokes equation (19th century) describes the rate of change of momentum at each point in a viscous fluid. The Navier-Stokes equation for a fluid with constant density ρ and constant kinematic viscosity ν is

$$\frac{\partial \mathbf{u}}{\partial t} + \mathbf{u} \cdot \nabla \mathbf{u} = -\frac{\nabla P}{\rho} + \nu \nabla^2 \mathbf{u} \quad , \qquad (1)$$

with $\nabla \cdot \mathbf{u} = 0$, which is a statement of fluid incompressibility and with suitable conditions imposed at the boundaries of the flow. The variable $\mathbf{u}(\mathbf{x},t)$ is the (incompressible) fluid velocity field, and $P(\mathbf{x},t)$ is the pressure field determined by the preservation of incompressibility. This equation (when multiplied by ρ to get force per unit volume) is simply Newton's law for a fluid: Force equals mass times acceleration. The left side of Equation (1) is the acceleration of the fluid,[2] and the right side is the sum of the forces per unit mass on a unit volume of the fluid:[3] the pressure force and the viscous force arising from momentum diffusion through molecular collisions. Remarkably, a simple equation representing a simple physical concept describes enormously complex phenomena.

The Navier-Stokes equations are deterministic in the sense that, once the initial flow and the boundary conditions are specified, the evolution of the state is completely determined, at least in principle. The nonlinear term in Equation (1), $\mathbf{u} \cdot \nabla \mathbf{u}$, describes the advective transport of fluid momentum. Solutions of the nonlinear Navier-Stokes equations may depend sensitively on the initial conditions so that, after a short time, two realizations of the flow with infinitesimally different initial conditions may be completely uncorrelated with each other. Changes in the external forcing or variations in the boundary conditions can produce flows that vary from smooth laminar flow to more complicated motions with an identifiable length or time scale, and from there to the most complicated flow of them all, namely, fully developed turbulence with its spectrum of motions over many length scales. Depending on the specific system (for example, flow in a pipe or behind a grid), the transition from smooth laminar flow to fully developed turbulence may occur abruptly, or by successively more complex states, as the forcing is increased.

The difficulties of finding solutions to the Navier-Stokes equations that accurately predict and/or describe the transition to turbulence and the turbulent state itself are legendary, prompting the British physicist Sir Horace Lamb to remark, "I am an old man

[1] Reynolds rewrote the Navier-Stokes fluid equation as two equations—one for the mean velocity, which includes a quadratic term in the fluctuating velocity called the Reynolds stress, and one for the fluctuations, which is usually modeled by some suitable approximation. This approach underpins commonly used engineering models of turbulent fluid motion known as Reynolds-Averaged Navier-Stokes (RANS)—refer to Taylor (1938).

[2] The acceleration term looks complicated because of the advection term $\mathbf{u} \cdot \nabla \mathbf{u}$, which arises from the coordinate transformation from a frame moving with the fluid parcels (the "Lagrangian" frame, in which Newton's law has the usual form) to a frame of reference fixed in space (the "Eulerian" frame, in which other aspects of the mathematics are simpler). Specifically, acceleration of the fluid is, by definition, the second time derivative of the Lagrangian fluid trajectory $\mathbf{x}(t)$, which describes the motion of the fluid element that was initially at position $\mathbf{x}(0)$. The first time derivative is the Lagrangian fluid velocity, $d\mathbf{x}(t)/dt$, which is related to the Eulerian fluid velocity by $d\mathbf{x}(t)/dt = \mathbf{u}(t,\mathbf{x}(t))$. Because $\mathbf{u}$ is a function of time t and position $\mathbf{x}(t)$, which itself is a function of time, the Eulerian expression for the Lagrangian second time derivative (the fluid acceleration) is obtained through the chain rule and equals $d\mathbf{u}/dt = \partial\mathbf{u}/\partial t + \mathbf{u} \cdot \nabla \mathbf{u}$.

[3] Often, there is an additional term added to the right side of the equation that represents an external forcing of the flow per unit volume such as by gravity. Alternatively, the forcing can arise from the imposition of boundary conditions, whereby energy is injected by stresses at those boundaries.

Figure 1. Common Examples of Fluid Turbulence

Turbulence is commonly apparent in everyday life, as revealed by the collage of pictures above: (a) water flow from a faucet, (b) water from a garden hose, (c) flow past a curved wall, and (d) and (e) whitewater rapids whose turbulent fluctuations are so intense that air is entrained by the flow and produces small bubbles that diffusely reflect light and cause the water to appear white.

now, and when I die and go to heaven there are two matters on which I hope for enlightenment. One is quantum electrodynamics, and the other is the turbulent motion of fluids. And about the former I am rather optimistic"—1932 (in Tannehill et al. 1984). One of the most influential turbulence theorists in the last 40 years, Robert Kraichnan, started studying turbulence while working with Albert Einstein at Princeton, when he noticed the similarity between problems in gravitational field theory and classical fluid dynamics. His contributions include field-theoretic approaches to turbulence that have had recent stunning success when applied to the turbulent transport of passive scalar concentration (see the article "Field Theory and Statistical Hydrodynamics" on page 181).

What Is Turbulence?

So, what is turbulence and why is it so difficult to describe theoretically? In this article, we shall ignore the transition to turbulence and focus instead on fully developed turbulence. One of the most challenging aspects is that, in fully developed turbulence, the velocity fluctuates over a large range of coupled spatial and temporal scales. Examples of turbulence (Figure 1) are everywhere: the flow of water from a common faucet, water from a garden hose, the flow past a curved wall, and noisy rapids resulting from flow past rocks in an energetically flowing river. Another example is the dramatic pyroclastic flow in a volcanic eruption. In Figure 2, the explosive eruption of Mount St. Helens is illustrated at successively higher magnification, showing structure at many length scales. In all these examples, large velocity differences (as opposed to large velocities) resulting from shear forces applied to the fluid (or from intrinsic fluid instability) produce strong fluid turbulence, a state that can be defined as a solution of the Navier-Stokes equations whose statistics exhibit spatial and temporal fluctuations.

Historically, investigations of turbulence have progressed through alternating advances in experimental measurements, theoretical descriptions, and most recently, the introduction of numerical simulation of turbulence on high-speed computers. Similarly, there has been a rich interplay between fundamental understand-

ing and applications. For example, turbulence researchers in the early to mid 20th century were motivated by two important practical problems: predicting the weather and building ever more sophisticated aircraft. Aircraft development led to the construction of large wind tunnels, where measurements of the drag and lift on scaled model aircraft were used in the design of airplanes. On the other hand, weather prediction was severely hampered by the difficulty in doing numerical computation and was only made practical after the development, many decades later, of digital computers; in the early days, the calculation of the weather change in a day required weeks of calculation by hand! In addition to these two large problems, many other aspects of turbulent flow were investigated and attempts were made to factor in the effects of turbulence on the design and operation of real machines and devices.

To understand what turbulence is and why it makes a big difference in practical situations, we consider flow through a long cylindrical pipe of diameter D, a problem considered over a century ago by Osborne Reynolds (1894). Reynolds measured mean quantities such as the average flow rate and the mean pressure drop in the pipe. A practical concern is to determine the flow rate, or mean velocity U, as a function of the applied pressure, and its profile, as a function of distance from the wall. Because the fluid is incompressible, the volume of fluid entering any cross section of the pipe is the same as the volume flowing out of the pipe. Thus, the volume flux is constant along the flow direction. We can use Equation (1) to get a naive estimate of the mean velocity U for flow in a horizontal pipe. Consider as a concrete example the flow of water in a rigid pipe hooked up to the backyard water faucet. Taking a 3-meter length of a 2.5-centimeter diameter pipe and estimating the water pressure at 30 pounds per square inch (psi), the imposed pressure gradient ∇P is 0.1 psi/cm or 7000 dynes/cm^3. We assume the simplest case, namely, that the flow is smooth, or "laminar," so that the nonlinear term in Equation (1) can be neglected, and that the flow has reached its limiting velocity with $\partial U/\partial t = 0$. In that case, the density-normalized pressure gradient $\nabla P/\rho$ would be balanced by the viscous acceleration (or drag), $\nu\nabla^2\mathbf{u}$. Using dimensional arguments and taking into account that $\mathbf{u} = 0$ at the pipe wall, we estimate that $\nu\nabla^2\mathbf{u} \approx \nu U/D^2$, which yields the estimate for the mean flow velocity of $U \sim \nabla P D^2/\rho\nu$. Thus, for water with viscosity $\nu = 0.01$ cm^2/s flowing in a pipe with diameter $D = 2.5$ centimeters, the laminar flow velocity would reach $U \sim 40{,}000$ m/s or almost 30 times the speed of sound in water! Clearly, something is wrong with this argument. It turns out that the flow in such a pipe is turbulent (it has highly irregular spatial and temporal velocity fluctuations) and the measured mean flow velocity U is smaller by a factor of about 4000, or only about 10 m/s!

How can we improve our estimate? For the turbulent case, we might assume, as Reynolds did, that the nonlinear term dominates over the viscous term and then equate the nonlinear term ($\mathbf{u} \cdot \nabla\mathbf{u} \sim U^2/D$) to the pressure gradient, thereby obtaining the much more realistic estimate of $U \sim (\nabla P D/\rho)^{1/2} \sim 1.5$ m/s. This estimate actually overestimates the effects of the nonlinear term.

As illustrated in Figure 3, the solution for the laminar-flow velocity profile is quite gradual, whereas the turbulent velocity profile is much steeper at the walls and levels off in the center of the pipe. Evidently, the effect of turbulence is to greatly increase the momentum exchange in the central regions of the pipe, as large-scale eddies effectively 'lock up' the flow and thereby shift the velocity gradient (or velocity shear) closer to the wall. Because the flow resistance in the pipe is proportional to the steepness of the velocity profile near the wall, the practical consequence of the turbulence is a large increase in the flow resistance of the pipe—that is, less flow for a given applied pressure. The real-world implications of this increase in flow resistance are enormous: A large fraction of the world's energy consumption is devoted to compensating for turbulent energy loss! Nevertheless, the detailed understanding and prediction from first principles still elude turbulence theory.

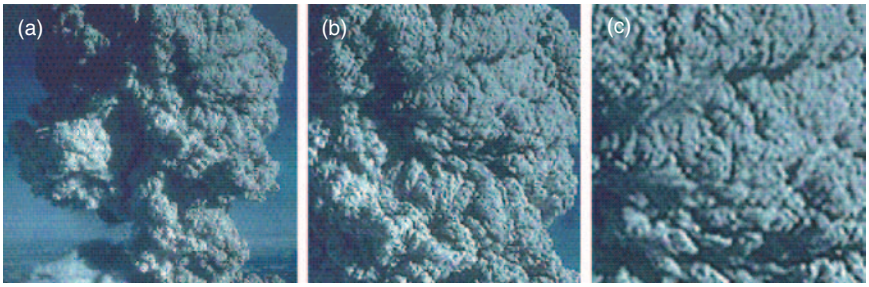

Figure 2. Scale-Independence in Turbulent Flows
The turbulent structure of the pyroclastic volcanic eruption of Mt. St. Helens shown in (a) is expanded by a factor of 2 in (b) and by another factor of 2 in (c). The characteristic scale of the plume is approximately 5 km. Note that the expanded images reveal the increasingly finer scale structure of the turbulent flow. The feature of scale independence, namely, that spatial images or temporal signals look the same (statistically) under increasing magnification is called self-similarity.

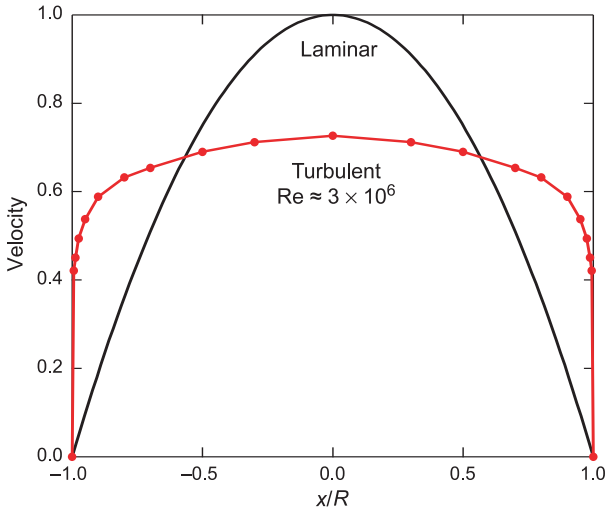

Figure 3. Mean Velocity Profiles for Laminar and Turbulent Pipe Flow
The velocity profile across the diameter ($D = 2R$ where R is the radius) of a pipe for laminar-flow conditions (black curve) shows a gradual velocity gradient compared with the very steep gradients near the walls resulting from turbulent flow conditions (red curve). Those steep gradients are proportional to the flow resistance in the pipe. Thus turbulence results in significantly less flow for a given applied pressure.

The example of pipe flow illustrates an important feature of turbulence—the ratio of the nonlinear term to the viscous dissipation term provides a good measure of the strength of turbulence. In fact, this ratio, $Re = UD/\nu$, where D is the size of the large-scale forcing (typically shear), is known as the Reynolds number after Reynolds' seminal work on pipe flow (1894). For a small Reynolds number, $Re << 1$, the nonlinearity can be neglected, and analytic solutions to the Navier-Stokes equation corresponding to laminar flow can often be found. When $Re >> 1$, however, there are no stable stationary solutions,[4] and the fluid flow is highly fluctuating in space and time, corresponding to turbulent flow. In particular, the flow is fully developed turbulence when Re is large compared with the Re for transition to turbulence for a particular set of forcing and boundary conditions. For example, in the problem above, where $D = 2.5$ cm and $U = 10$ m/s, the Reynolds number is $Re \sim 3 \times 10^5$ compared with a typical $Re \sim 2000$ for the onset of turbulence in pipe flow.

The Search for Universal Properties and the Kolmogorov Scaling Laws

In early laboratory experiments on turbulence, Reynolds and others supplemented their measurements of applied pressure and average velocity by observing the rapidly fluctuating character of the flow when they used dyes and other qualitative flow-visualization tools. In the atmosphere, however, one could measure much longer-term fluctuations, at a fixed location, and such Eulerian measurements intrigued the young theoretical physicist G. I. Taylor (1938). Turbulence is difficult to measure because the turbulent state changes rapidly in space and time. Taylor proposed a probabilistic/statistical approach based on averaging over ensembles of individual realizations, although he soon replaced ensemble averages by time averages at a fixed point in space. Taylor also used the idealized concept (originally introduced by Lord Kelvin in 1887) of statistically homogeneous, isotropic turbulence. Homogeneity and isotropy imply that spatial translations and rotations, respectively, do not change the average values of physical variables.[5]

Lewis F. Richardson was another influential fluid dynamicist of the early 20th century. Richardson performed the first numerical computation for predicting the weather (on a hand calculator)! He also proposed (1926) a pictorial description of turbulence called a cascade, in which nonlinearity transforms large-scale velocity circulations (or eddies, or whorls) into circulations at successively smaller scales (sizes) until they reach such a small scale that the circulation of the eddies is efficiently dissipated into heat by viscosity. Richardson captured this energy cascade in a poetic take-off on Jonathan Swift's famous description of fleas.[6] In Richardson's words, "Big whorls have little whorls that feed on their velocity, and little whorls have lesser whorls and so on to viscosity" (circa 1922). A schematic illustration of the energy cascade picture is shown in Figure 4, where the mean energy

[4] How large Re must be to get a turbulent state depends on the particular source of forcing and on the boundary conditions. For example, the transition to turbulence in pipe flow can occur anywhere in the range $1000 < Re < 50{,}000$ depending on inlet boundary conditions and the roughness of the pipe wall. For most commonly encountered conditions, the transition is near $Re = 2000$.

[5] Many theoretical descriptions use these assumptions, but typical turbulence encountered in the real world often obeys neither condition at large scales. A key question in real-world situations is whether the assumptions of homogeneity and isotropy are satisfied at small scales, thus justifying application of a general framework for those smaller scales.

[6] "So, the naturalists observe, the flea,/ hath smaller fleas that on him prey;/ And these have smaller still to bite 'em;/ And so proceed, ad infinitum."—Jonathan Swift, *Poetry, a Rhapsody*

injection rate ε at large scales is balanced by the mean energy dissipation rate at small scales. Richardson and Taylor also appreciated that generic properties of turbulence may be discovered in the statistics of velocity differences between two locations separated by a distance **r**, denoted as $\delta\mathbf{u}(\mathbf{x}, \mathbf{x}+\mathbf{r}) = \mathbf{u}(\mathbf{x}) - \mathbf{u}(\mathbf{x}+\mathbf{r})$. The statistics of velocity differences at two locations are an improvement over the statistics of velocity fluctuations at a single location for a number of technical reasons, which we do not discuss here. Longitudinal projections of velocity differences

$$\delta u(r) = \delta\mathbf{u}(\mathbf{x}, \mathbf{x}+\mathbf{r}) \cdot \mathbf{r} / |\mathbf{r}|$$

are often measured in modern experiments and are one of the main quantities of interest in the analysis of fluid turbulence.

Measuring velocity differences on fast time scales and with high precision was a difficult proposition in the early 20th century and required the development of the hot-wire anemometer, in which fluid flowing past a thin heated wire carries heat away at a rate, proportional to the fluid velocity. Hot-wire anemometry made possible the measurement, on laboratory time scales, of the fluctuating turbulent velocity field at a single point in space (see Figure 5). For a flow whose mean velocity is large, velocity differences were inferred from those single-point measurements by Taylor's "frozen-turbulence" hypothesis.[7]

[7] If the mean velocity is large compared with velocity fluctuations, the turbulence can be considered "frozen" in the sense that velocity fluctuations are swept past a single point faster than they would change because of turbulent dynamics. In that case, the spatial separation Δr is related to the time increment Δt by $\Delta r = -U\Delta t$, where U is the mean velocity. See also the article "Taylor's Hypothesis, Hamilton's Principle, and the LANS-α Model for Computing Turbulence" on page 152 .

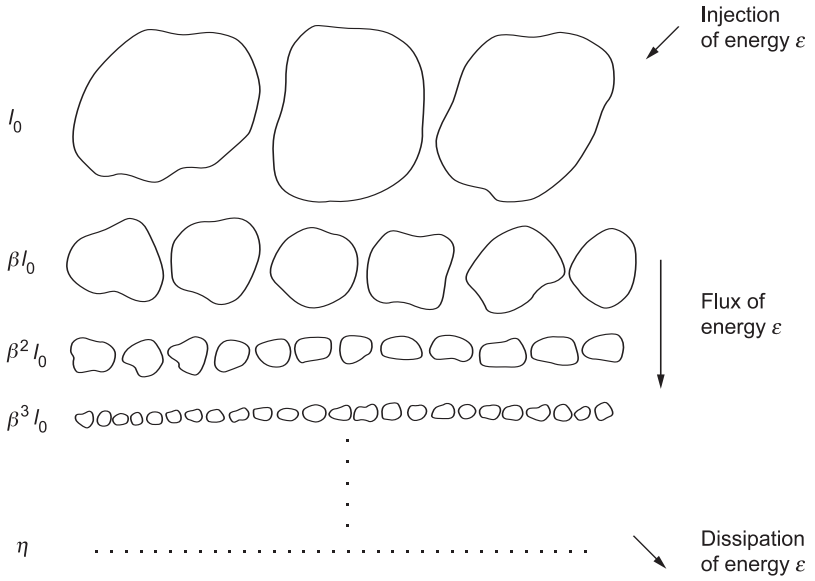

Figure 4. The Energy Cascade Picture of Turbulence
This figure represents a one-dimensional simplification of the cascade process with β representing the scale factor (usually taken to be 1/2 because of the quadratic nonlinearity in the Navier-Stokes equation). The eddies are purposely shown to be "space filling" in a lateral sense as they decrease in size.
(This figure was modified with permission from Uriel Frisch. 1995. *Turbulence*: *The Legacy of A. N. Kolmogorov*. Cambridge, UK: Cambridge University Press.)

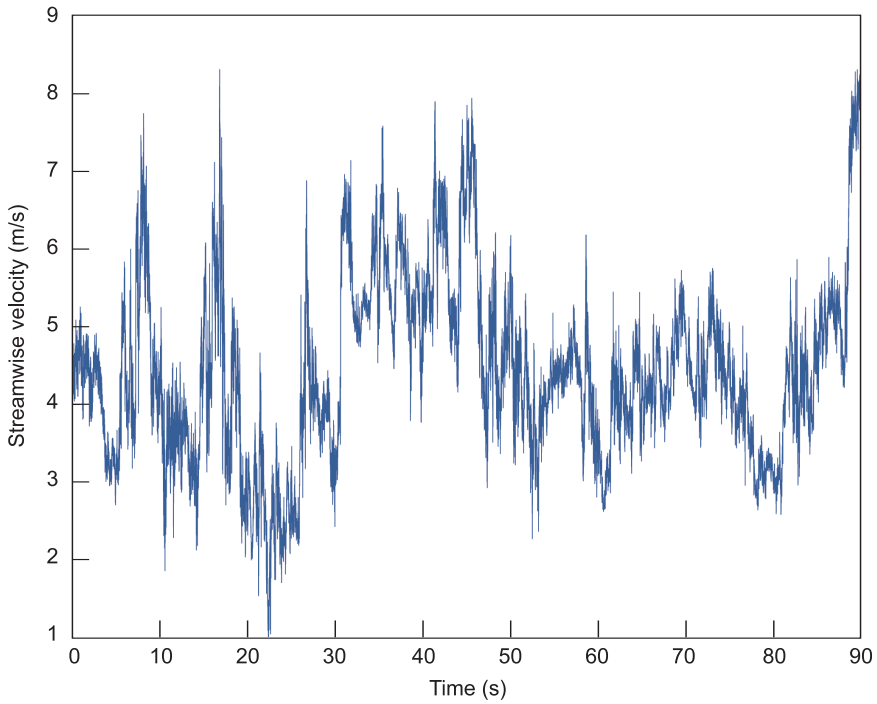

Figure 5. Time Series of Velocities in a Turbulent Boundary Layer
This time series of velocities for an atmospheric turbulent boundary layer with Reynolds number $Re \sim 2 \times 10^7$ was measured at a single location with a hot-wire anemometer. The velocity fluctuations are apparently random. (This figure is courtesy of Susan Kurien of Los Alamos, who has used data recorded in 1997 by Brindesh Dhruva of Yale University.)

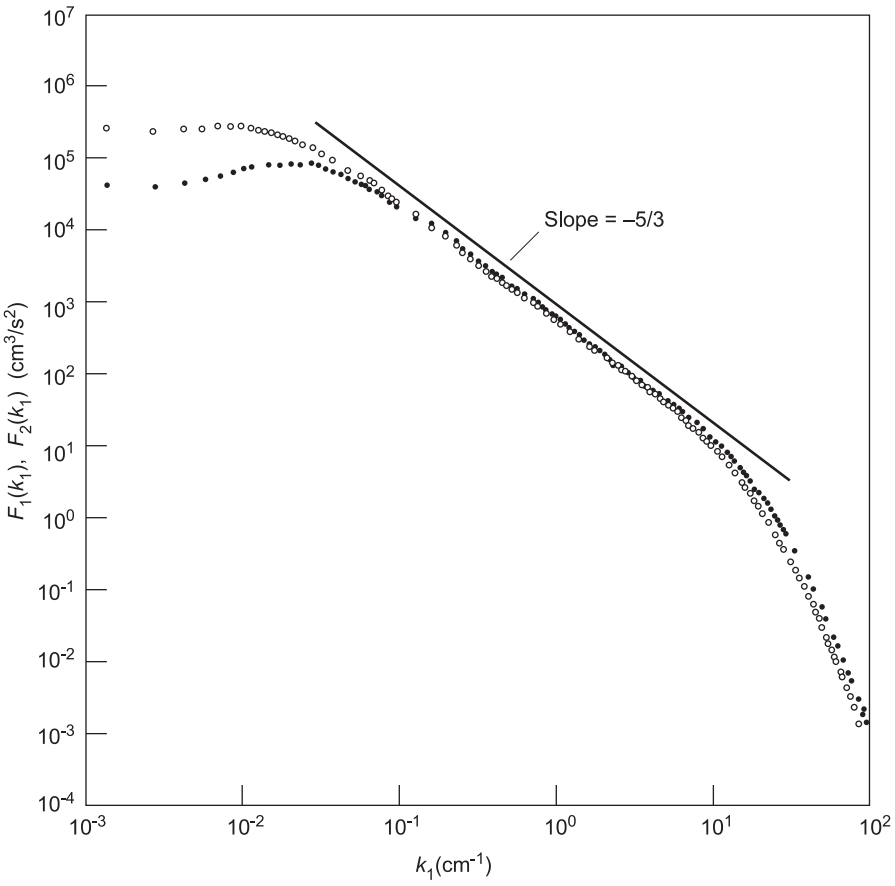

Figure 6. Kolmogorov-like Energy Spectrum for a Turbulent Jet
The graph shows experimental data for the energy spectrum (computed from velocity times series like that in Figure 5) as a function of wave number *k*, or *E*(*k*) vs *k*, for a turbulent jet with Reynolds number *Re* ~ 24,000. Note that the measured spectrum goes as $E(k) \propto k^{-5/3}$. (Champagne 1978. Redrawn with the permission of Cambridge University Press.)

Single-point measurements of turbulent velocity fluctuations have been performed for many systems and have contributed both to a fundamental understanding of turbulence and to engineering modeling of the effects of turbulence at small scales on the flow at larger scales. (See the section on engineering models.) Single-point measurements of velocity fluctuations have been the primary tool for investigating fluid turbulence.They remain in common use because of their large dynamic range and high signal-to-noise ratio relative to more modern developments such as particle image velocimetry, in which the goal is to measure whole velocity fields. For now, we consider results that were motivated or measured with the limitations of single-point experiments in mind.

The Kolmogorov Scaling Laws. In 1938, von Kármán and Howarth derived an exact theoretical relation for the dynamics of turbulence statistics. Starting from the Navier-Stokes equation and assuming homogeneity and isotropy, the two scientists derived an equation for the dynamics of the lowest-order two-point velocity correlation function. (This function is $\langle \mathbf{u}(\mathbf{x}) \cdot \mathbf{u}(\mathbf{x}+\mathbf{r}) \rangle$, where the angle brackets denote an ensemble average, that is, an average over many statistically independent realizations of the flow. The two-point velocity correlation functions cannot describe universal features of turbulence because they are scale dependent (the large-scale flow dominates their behavior) and they lack Galilean invariance. Nevertheless, their derivation inspired a real breakthrough. In 1941, Andrei Kolmogorov recast the Kármán-Howarth equation in terms of the moments of $\delta u(r)$, the velocity differences across scales, thereby producing a relationship between the second moment $\langle [\delta u(r)]^2 \rangle$ and the third moment $\langle [\delta u(r)]^3 \rangle$. These statistical objects, which retain Galilean invariance and hence hold the promise of universality, are now known as structure functions.

Kolmogorov then proposed the notion of an "inertial range" of scales based on Richardson's picture of the energy cascade: Kinetic energy is injected at the largest scales L of the flow at an average rate ε and generates large-scale fluctuations. The injected energy cascades to smaller scales via nonlinear inertial (energy-conserving) processes until it reaches a scale of order ℓ_d, where viscous dissipation becomes dominant and the kinetic energy is converted into heat. In other words, the intermediate spatial scales r, in the interval $\ell_d << r << L$, define an inertial range in which large-scale forcing and viscous forces have negligible effects. With these assumptions and the Kármán-Howarth equation recast for structure functions, Kolmogorov derived the famous "four-fifths law." The equation defining this law describes an exact relationship for the third-order structure function within the inertial range:

$$\left\langle \left[\delta u(r)\right]^3 \right\rangle = -(4/5)\varepsilon r \ ,$$

where ε is assumed to be the finite energy-dissipation rate (per unit mass) of the turbulent state. This relation-

ship is a statement of conservation of energy in the inertial range of scales of a turbulent fluid; the third moment, which arises from the nonlinear term in Equation (1), is thus an indirect measure of the flux of energy through spatial scales of size r. (High Reynold's-number numerical simulations are compared with the four-fifths law and with other statistical characterizations of turbulence in the article "Direct Numerical Simulations of Turbulence" on page 142.)

Kolmogorov further assumed that the cascade process occurs in a self-similar way. That is, eddies of a given size behave statistically the same as eddies of a different size. This assumption, along with the four-fifths law, gave rise to the general scaling prediction of Kolmogorov, which states that the nth order structure function (referred to in the article "Direct Numerical Simulations of Turbulence" as $S_n(r)$) must scale as $r^{n/3}$. During the decades that have passed since Kolmogorov's seminal papers (1941), empirical departures from his scaling prediction have been measured for n different from 3, leading to our present understanding that turbulent scales are not self-similar, but that they become increasingly intermittent as the scale size decreases. The characterization and understanding of these deviations, known as the "anomalous" scaling feature of turbulence, have been of sustained and current interest (see the box "Intermittency and Anomalous Scaling in Turbulence" on page 136).

Empirical observations show that a flow becomes fully turbulent only when a large range of scales separates the injection scale L and the dissipation scale ℓ_d. A convenient measure of this range of spatial scales for fluid turbulence, which also characterizes the number of degrees of freedom of the turbulent state, is the large-scale Reynolds number, Re. The Reynolds number is also the ratio of nonlinear to viscous forces introduced earlier in the context of pipe flow. Most theories of turbulence deal with asymptotically large Re, that is, $Re \to \infty$, so that an arbitrarily large range of scales separates the injection scales from the dissipation scales.

Because energy cascading down through spatial scales is a central feature of fluid turbulence, it is natural to consider the distribution of energy among spatial scales in wave number (or Fourier) space, as suggested by Taylor (1938). The energy distribution $E(\boldsymbol{k}) = 1/2|\tilde{\mathbf{u}}(\mathbf{k})|^2$, where $\tilde{\mathbf{u}}(\mathbf{k})$ is the Fourier transform of the velocity field and the wave number k is related to the spatial scale ℓ by $k = 2\pi/\ell$.[8] Wave-number space is very useful for the representation of fluid turbulence because differential operators in real space transform to multiplicative operators in k-space. For example, the diffusion operator in the term $\nu\nabla^2\mathbf{u}$ becomes $\nu k^2\tilde{\mathbf{u}}$ in the Fourier representation. Another appealing feature of the wave number representation is the nonlocal property of the Fourier transform, which causes each Fourier mode represented by wave number k to represent cleanly the corresponding scale ℓ. On the other hand, the k-space representation is difficult from the perspective of understanding how spatial structures, such as intense eddies, affect the transfer of energy between scales, that is between eddies of different sizes.

The consequence of energy conservation on the form of $E(k)$ was independently discovered by Obukov (1941), Heisenberg (1948), and Onsager (1949), all of whom obtained the scaling relationship for the energy spectrum $E(k) \sim k^{-5/3}$ for the inertial scales in fully developed homogeneous isotropic turbulence. This result is not independent of the picture presented above in terms of real space-velocity differences but is another way of looking at the consequences of energy conservation. Many subsequent experiments and numerical simulations have observed this relationship to within experimental/numerical uncertainty, thereby lending credence to the energy cascade picture. Figure 6 shows the energy spectrum obtained from time series measurements at a single point in a turbulent jet, where the spatial scale is related to time by Taylor's hypothesis that the large mean velocity sweeps the "frozen-in" turbulent field past the measurement point.

Vorticity. Another important quantity in the characterization and understanding of fluid turbulence is the vorticity field, $\boldsymbol{\omega}(x,t) = \nabla \times \mathbf{u}(x,t)$, which roughly measures the local swirl of the flow as picturesquely drawn by da Vinci in the opening illustration. The notion of an "eddy" or "whorl" is naturally associated with one's idea of a vortex—a compact swirling object such as a dust devil, a tornado, or a hurricane—but this association is schematic at best. In three-dimensional (3-D) turbulence, vorticity plays a quantitative role in that the average rate of energy dissipation ε is related to the mean-square vorticity by the relation $\varepsilon = -u\langle |\boldsymbol{\omega}|^2\rangle$. Vorticity plays a different role in two-dimensional (2-D) turbulence. Vortex stretching has long been recognized as an important ingredient in fluid turbulence (Taylor 1938); if a vortex tube is stretched so that its cross section is reduced, the mean-square vorticity in that cross section will increase, thereby causing strong spatially localized vortex filaments that dissipate energy. The notion of vortex stretching and energy dissipation is discussed in the article "The LANS-α model for Computing Turbulence" on page 152.

[8] If isotropy is assumed, the energy distribution $E(\mathbf{k})$, where $\mathbf{k}$ is a vector quantity, depends only on the magnitude $k = |\mathbf{k}|$ and one can denote the energy as $E(k)$ without loss of generality.

Engineering Models of Turbulence

It is worth stressing again that turbulence is both fundamentally interesting and of tremendous practical importance. As mentioned above, modeling complex practical problems requires a perspective different from that needed for studying fundamental issues. Foremost is the ability to get fairly accurate results with minimal computational effort. That goal can often be accomplished by making simple models for the effects of turbulence and adjusting coefficients in the model by fitting computational results to experimental data. Provided that the parameter range used in the model is well covered by experimental data, this approach is very efficient. Examples that have benefited from copious amounts of reliable data are aircraft design—aerodynamics of body and wing design have been at the heart of a huge international industry—and aerodynamic drag reduction for automobiles to achieve better fuel efficiency. Global climate modeling and the design of nuclear weapons, on the other hand, are examples for which data are either impossible or quite difficult to obtain. In such situations, the utmost care needs to be taken when one attempts to extrapolate models to circumstances outside the validation regime.

The main goal of many engineering models is to estimate transport properties—not just the net transport of energy and momentum by a single fluid but the transport of matter such as pollutants in the atmosphere or the mixing of one material with another. Mixing is a critical process in inertial confinement fusion and in weapons physics applications. It is crucial for certification of the nuclear weapons stockpile that scientists know how well engineering models are performing and use that knowledge to predict outcomes with a known degree of certainty.

The Closure Problem for Engineering Models. Engineering models are constructed for computational efficiency rather than perfect representation of turbulence. The class of engineering models known as Reynolds-Averaged Navier-Stokes (RANS) provides a good example of how the problem of "closure" arises and the parameters that need to be determined experimentally to make those models work. Consider again the flow of a fluid with viscosity ν in a pipe with a pressure gradient along the pipe. When the pressure applied at the pipe inlet and the pipe diameter D are small, the fluid flow is laminar, and the velocity profile in the pipe is quadratic with a peak velocity U that is proportional to the applied pressure (refer to Figure 3). When the forcing pressure gets large enough to produce a high flow velocity and therefore a large Reynolds number, typically $Re = UD/\nu \geq 2000$, the flow becomes turbulent, large velocity fluctuations are present in the flow, and the velocity profile changes substantially (refer again to Figure 3). An engineering challenge is to compute the spatial distribution of the mean velocity of the turbulent flow. Following the procedure first written down by Reynolds, the velocity and pressure fields are separated into mean (the overbar denotes a time average) and fluctuating (denoted by the prime) parts:

$$u_i(\mathbf{x},t) = \bar{u}_i(\mathbf{x},t) + u_i'(\mathbf{x},t) \ ,$$

where i denotes one of the components of the vector field $\mathbf{u}(x,t)$ and the average of the fluctuating part of the velocity is zero by definition. Also,

$$P(\mathbf{x},t) = \bar{P}(\mathbf{x},t) + P'(\mathbf{x},t) \ .$$

Substituting these expressions into Equation (1), using the constant-density continuity condition

$$\nabla \cdot \mathbf{u} = 0 \Rightarrow \nabla \cdot \bar{\mathbf{u}} = 0 = \nabla \cdot \mathbf{u}' \ ,$$

and averaging term by term yields an equation for the mean velocity:

$$\frac{\partial \bar{u}_i}{\partial t} + \bar{u}_j \frac{\partial \bar{u}_i}{\partial x_j} + \frac{\partial \overline{u_i' u_j'}}{\partial x_j} = -\frac{1}{\rho}\frac{\partial \bar{P}}{\partial x_i} + \nu \frac{\partial^2 \bar{u}_i}{\partial x_j^2} \ . \quad (2)$$

Note that the equation for the mean flow looks the same as the Navier-Stokes equation for the full velocity **u**, Equation (1), with the addition of a term involving the time average of a product of the fluctuating parts of the velocity, namely, the Reynolds stress tensor,

$$R_{ij} = \overline{u_i' u_j'} \ ,$$

That additional term, which represents the transport of momentum caused by turbulent fluctuations, acts like an effective stress on the flow and cannot, at this time, be determined completely from first principles. As a result, many schemes have been developed to approximate the Reynolds stress.

The simplest formulation for the Reynolds stress tensor is

$$R_{ij} = -\nu_T(x)\frac{\partial \bar{u}_i}{\partial x_j} \ ,$$

where $\nu_T(x)$ is called the turbulent eddy viscosity because the additional term looks like a viscous diffusion term. A more sophisticated approach is to solve for the Reynolds stress by writing an equation for the time evolution of $\overline{u_i' u_j'}$ (Johnson et al. 1986). This equation has multiple undetermined coefficients and depends on the third moment $\overline{u_i' u_j' u_k'}$. Again, the third-order moment is unknown and needs to be approximated or written in terms of fourth-order moments. In principle, an infinite set of equations for higher-order moments is required, so one needs to "close" the set at a small number to achieve computational effi-

ciency. At any stage of approximation, undetermined coefficients are set by comparison with experimental or direct numerical simulation data. This approach is often very effective, although it does depend on the quality of the data and on the operating parameter regime covered by the data.

Modern Developments

By the end of the 1940s, great progress had been made in the study of turbulence. The statistical approach to turbulence, the importance of the energy and its wave number representation, the notion of measuring velocity differences, and the dynamics of vortex structures as an explanation of the mechanism of fluid turbulence had all been articulated by Taylor. The cascade picture of Richardson had been made quantitative by Kolmogorov and others. The concepts of universal scaling and self-similarity were key ingredients in that description. On the practical side, tremendous advances had been made in aeronautics, with newly emerging jet aircraft flying at speeds approaching the speed of sound. Empirical models based on the engineering approach described above were being used to describe these practical turbulence problems.

The next 50 years were marked by steady progress in theory and modeling, increasingly sophisticated experiments, and the introduction and widespread use of the digital computer as a tool for the study of turbulence. In the remainder of this review, we touch on some of the advances of the post-Kolmogorov era, paying particular attention to the ever-increasing impact of the digital computer on three aspects of turbulence research: direct numerical simulations of idealized turbulence, increasingly sophisticated engineering models of turbulence, and the extraordinary enhancement in the quality and quantity of experimental data achieved by computer data acquisition. As far back as the Manhattan Project, the computer (more exactly, numerical schemes implemented on a roomful of Marchand calculators) began to play a major role in the calculations of fluid problems. A leading figure in that project, John von Neumann (1963), noted in a 1949 review of turbulence that "… a considerable mathematical effort towards a detailed understanding of the mechanism of turbulence is called for" but that, given the analytic difficulties presented by the turbulence problem, "… there might be some hope to 'break the deadlock' by extensive, but well-planned, computational efforts." Von Neumann's foresight in understanding the important role of computers for the study of turbulence predated the first direct numerical simulation of the turbulent state by more than 20 years.

From a fundamental perspective, the direct numerical simulation of idealized isotropic, homogeneous turbulence has been revolutionary in its impact on turbulence research because of the ability to simulate and display the full 3-D velocity field at increasingly large Reynolds number. Similarly, experimentation on turbulence has advanced tremendously by using computer data acquisition; 20 years ago it was possible to measure and analyze time series data from single-point probes that totaled no more than 10 megabytes of information, whereas today statistical ensembles of thousands of spatially and temporally resolved velocity fields, taking 10 terabytes of storage space can be obtained and processed. This millionfold increase in experimental capability has opened the door to great new possibilities in turbulence research that will be enhanced even further by expected future increases in computational power.

Below, we briefly address advances in numerical simulation, in turbulence modeling, and theoretical understanding of passive scalar transport, topics dealt with more extensively in the articles immediately following this one. We then describe several exciting new experimental advances in fluid turbulence research and close this introduction with a view toward "solving" at least some aspect of the turbulence problem.

Direct Numerical Simulation of Turbulence

Recent advances in large-scale scientific computing have made possible direct numerical simulations of the Navier-Stokes equation under turbulent conditions. In other words, for simulations performed on the world's largest supercomputers, no closure or subgrid approximations are used to simplify the flow, but rather the simulated flow follows all the twisting-turning and stretching-folding motions of the full-blown Navier-Stokes equations at effective large-scale Reynolds numbers of about 10^5. These simulations render available for analysis the entire 3-D velocity field down to the dissipation scale. With these numerically generated data, one can study the structures of the flow and correlate them with turbulent transfer processes, the nonlinear processes that carry energy from large to small scales.

An especially efficient technique for studying isotropic, homogeneous turbulence is to consider the flow in a box of length L with periodic boundary conditions and use the spectral method, an orthogonal decomposition into Fourier modes, to simulate the Navier-Stokes equation. Forcing is typically generated by maintaining constant energy in the smallest k mode (or a small number of the longest-wavelength modes).

The first direct numerical simulation of fluid turbulence (Orszag and Patterson 1972) had a resolution of 32^3, corresponding to $Re \sim 100$. By the early 1990s, Reynolds numbers of about 6000 for a 512^3 simulation could be obtained (She et al. 1993); the separation between the box size and the dissipation scale was just short of a decade. Recent calculations on the Los Alamos Q machine, using 2048^3 spatial resolution, and on the Japanese Earth Simulator with 4096^3 modes (Kaneda et al. 2003) achieved a Reynolds number of about 10^5, corresponding to about 1.5 decades of turbulent scales, which is approaching fully developed turbulence in modestly sized wind tunnels. It is important to appreciate that the *Re* of direct numerical turbulence simulations grows only as $Re \propto N^{4/9}$, where N is the number of degrees of freedom that are computed: A factor of 2 increase in the linear dimension of the box means computing 2^3 more modes for a corresponding increase in *Re* of about 2.5. Nevertheless, for isotropic, homogeneous fully developed turbulence, direct numerical simulation has become the tool of choice for detailed characterization of fundamental flow properties and comparison with Kolmogorov-type theories. More details regarding numerical simulation of turbulence can be found in the article "Direct Numerical Simulations of Turbulence" on page 142.

Modern Turbulence Models

Although the RANS models described above maintain a dominant role in turbulence modeling, other approaches have become tractable because of increases in computational power. A more recent approach to modeling turbulent processes is to decompose spatial scales of the flow into Fourier modes and then to truncate the expansion at some intermediate scale (usually with a smooth Gaussian filter) and model the small scales with a subgrid model. One then computes the large scales explicitly and approximates the effect of the small scales with the subgrid model. This class of methods (Meneveau and Katz 2000) is called large eddy simulation (LES) and has become an alternative to RANS modeling when more-accurate spatial information is required. Because of the spatial filtering, LES modeling has problems with boundaries and is less computationally efficient than RANS techniques. Nevertheless, LES models may be more universal than RANS models and therefore rely less on ad hoc coefficients determined from experimental data.

Another variant of the subgrid-model approach recently invented at Los Alamos is the Lagrangian-averaged Navier-Stokes alpha (LANS-α) model. Although not obtainable by filtering the Navier-Stokes equations, the LANS-α model has a spatial cutoff determined by the coefficient α. For spatial scales larger than α, the dynamics are computed exactly (in effect, the Navier-Stokes equations are used) and yield the energy spectrum $E(k) \propto k^{-5/3}$, whereas for spatial scales less than α, the energy falls more rapidly, $E(k) \propto k^{-3}$. The LANS-α model can be derived from a Lagrangian-averaging procedure starting from Hamilton's principle of least action. It is the first-closure (or subgrid) scheme to modify the nonlinear term rather than the dissipation term and, as a result, has some unique advantages relative to more traditional LES schemes (see the articles "The LANS-α Model for Computing Turbulence" and "Taylor's Hypothesis, Hamilton's Principle, and the LANS-α Model for Computing Turbulence" on pages 152 and 172, respectively).

Beyond the Kolmogorov Theory

The 50 years that have passed, from about 1950 until the new millennium, were notable for increasingly sophisticated theoretical descriptions of fluid turbulence, including the seminal contributions of Robert Kraichnan (1965, 1967, 1968, 1975), who pioneered the foundations of the modern statistical field-theory approach to hydrodynamics, particularly by predicting the inverse energy cascade from small scales to large scales in 2-D turbulence, and George Batchelor (1952, 1953, 1959, 1969). Those developments are generally beyond the scope of the present review, and we have already referred the reader to recent books in which they are surveyed in detail (McComb 1990, Frisch 1995, Lesieur 1997). We touch briefly, however, on a few recent developments that grew out of those efforts and on the influence of the Lagrangian perspective of fluid turbulence.

The physical picture that emerges from the Kolmogorov phenomenology is that the turbulent scales of motion are self-similar; that is, the statistical features of the system are independent of spatial scale. One measure of this self-similarity is the nondimensional ratio of the fourth moment to the square of the second moment, $F = \langle \delta u^4 \rangle / \langle \delta u^2 \rangle^2$, as a function of scale separation. If the velocity distribution is self-similar, then F should be constant, or flat, as a function of length scale. Indeed, the nondimensional ratio of any combination of velocity-increment moments should be scale independent. If, however, F behaves as a power law in the separation r, then the system is not self-similar, but instead it is characterized by intermittency: short bursts (in time) or isolated regions (in space) of high-amplitude fluctuations separated by relatively quiescent periods or

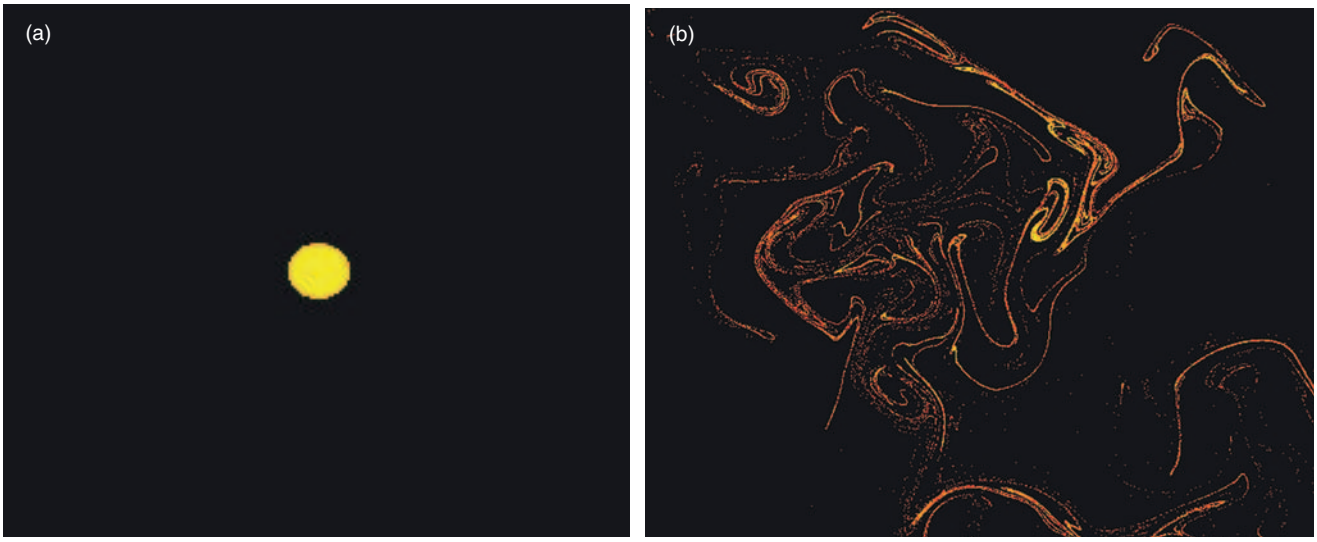

Figure 7. Passive Scalar Turbulence in a Stratified Layer
An effective blob of yellow dye is carried by a forced 2-D turbulent flow in a stratified layer. The images show (a) the initial dye concentration and (b) the concentration after about one rotation of a large-scale eddy. The sharp gradients in the concentration lead to the very strong anomalous scaling in the transport of the passive scalar field.

regions. From the 1960s to the 1980s, experimentalists reported departures from the Kolmogorov scaling. The measured fourth-order and higher moments of velocity differences did not scale as $r^{n/3}$, but rather as a lower power of the separation r, $\langle \delta u^n \rangle \sim r^{\xi_n}$, with $\xi_n < n/3$ for $n > 3$. To preserve the correct dimensions of the nth-order velocity difference moments, the deviations from Kolmogorov scaling, or from self-similarity, can be written as a correction factor given by the ratio of the large scale L to the separation r to some power Δ_n, or $(L/r)^{\Delta_n}$ (see the box "Intermittency and Anomalous Scaling in Turbulence" on page 136). Some recent analytic progress toward understanding the origin of the observed anomalous scaling has been made in the context of passive scalar turbulence and involves the application of nonperturbative field-theory techniques to that problem (see the article "Field Theory and Statistical Hydrodynamics" on page 181).

The passive scalar problem describes the transport and effective diffusion of material by a turbulent velocity field. This stirring process characterizes fluid mixing, which has many important scientific and technical applications. Whereas intermittency is rather weak in turbulent velocity statistics, the distribution of a passive scalar concentration carried by a turbulent flow is very intermittent. In other words, there is a much larger probability (compared with what one would expect for a random, or Gaussian, distribution) of finding local concentrations that differ greatly from the mean value. For characterizing fluid mixing, the Lagrangian frame of reference (which moves with the fluid element as opposed to the Eulerian frame, which is fixed in space) is very useful theoretically because a passive scalar is carried by fluid elements. Figure 7 shows the distribution of a virtual drop of yellow dye carried by a 2-D turbulent flow in a stratified layer experiment.[9] The structured distribution of the dye illustrates how the velocity field stretches and folds fluid elements to produce mixing. Adopting the Lagrangian frame of reference is rapidly emerging as a powerful new approach for modeling turbulent mechanisms of energy transfer. This approach has led to Lagrangian tetrad methods, a phenomenological model arising from the nonperturbative field-theoretical approach to turbulence, and to the LANS-α model mentioned above.

[9]The "virtual" drop consists of more than 10,000 fluid elements, whose evolution is computed by solving the Lagrangian equation $d\mathbf{x}(t)/dt = \mathbf{u}(t,\mathbf{x}(t))$ from experimental velocity fields.

Recent Experimental Developments

Quantitative single-point measurements of velocity combined with qualitative flow visualization (van Dyke 1982) have characterized almost all experimental measurements of fluid turbulence for most of the 20th century. Recently, however, new experimental techniques enabled by digital data acquisition, powerful pulsed-laser technology, and fast digital imaging systems have emerged and are causing great excitement in the field of turbulence.

Intermittency and Anomalous Scaling in Turbulence

Misha Chertkov

Intermittency is associated with the violent, atypical discontinuous nature of turbulence. When a signal from turbulent flow (for example, the velocity along a particular direction) is measured at a single spatial point and a sequence of times (an Eulerian measurement), the fluctuations in the values appear to be random. Since any random sequence is most naturally explained in terms of its statistical distribution, one typically determines the statistics by constructing a histogram of the signal. The violent nature of turbulence shows itself in the very special shape of the histogram, or the probability distribution function (PDF), of the turbulent velocity signal. It is typically wider than the Gaussian distributions emerging in the context of equilibrium statistical physics—for example, the Gaussian distribution that describes the velocity of (or the distance traveled by) a molecule undergoing Brownian motion.

The PDF of the energy dissipation rate, $P(\varepsilon)$, illustrates how far from Gaussian a turbulent distribution can be. At values far above the average, $\varepsilon >> \langle\varepsilon\rangle$, where $\varepsilon \equiv \nu(\nabla u)^2$, the probability distribution $P(\varepsilon)$ has a stretched exponential tail, $\ln P(\varepsilon) \propto -\varepsilon^a$ (La Porta 2001). The extended tail of the turbulent PDF illustrates the important role played by the atypical, violent, and rare events in turbulence.

Intermittency has many faces. In the context of two-point measurements, intermittency is associated with the notion of anomalous scaling. Statistics of the longitudinal velocity increments, $\delta u(r)$ (the difference in the velocity components parallel to the line separating the two points) in developed turbulence becomes extremely non-Gaussian as the scale decreases. In particular, if the scale r separating the two points is deep inside the inertial interval, $L >> r >> \ell_{\mathrm{d}}$, then the nth moment of the longitudinal velocity increment is given by

$$\left\langle [\delta u(r)]^n \right\rangle \approx \langle\varepsilon\rangle^{n/3} r^{n\alpha/3} \left(L/r\right)^{\Delta_n} , \qquad (1)$$

where L is the integral (pumping, energy-containing) scale of turbulence. The first thing to mention about Equation (1) is that the viscous, Kolmogorov scale ℓ_{d} does not enter the relation in the developed turbulence regime. This fact is simply related to the direction of the energy cascade: On average, energy flows from the large scale, where it is pumped into the system, toward the smaller scale, ℓ_{d}, where it is dissipated; it does not flow from the small scale. Secondly, Δ_n on the right side of Equation (1) is the anomalous scaling exponent. In the phenomenology proposed by Kolmogorov in 1941, the flow is assumed to be self-similar in the inertial range of scales, which implies that anomalous scaling is absent, $\Delta_n = 0$, for all values of n. The self-similar scaling phenomenology is an extension of the four-fifths law proven by Kolmogorov in 1941 for the third moment

$$\left\langle [\delta u(r)]^3 \right\rangle = -\frac{4}{5}\langle\varepsilon\rangle r \ .$$

(See discussion of the four-fifths law in "Direct Numerical Simulations of Turbulence" on page 142). This law is a statement of conservation of energy from scale to scale in the inertial regime of homogeneous isotropic turbulence. Modern experimental and numerical tests (Frisch 1995) unequivocally dismiss the self-similarity assumption, $\Delta_n = 0$, as invalid. But so far, theory is still incapable of adding any other exact relation to the celebrated four-fifths law.

On the other hand, even though a comprehensive theoretical analysis of developed isotropic turbulence remains elusive, there has been an important breakthrough in understanding anomalous scaling in the simpler problem of passive scalar turbulence (see the article "Field Theory and Statistical Hydrodynamics" on page 181).

One innovative example of a new turbulence experiment (La Porta 2001) is the use of silicon strip detectors from high-energy physics to track a single small particle in a turbulent flow with high Reynolds number (see Figure 8). This is an example of the direct measurement of Lagrangian (moving with the fluid) properties of the fluid flow. Because the particle trajectories are time resolved, the acceleration statistics can be obtained directly from experiment, and theoretical predictions for those statistics can be tested.

Another application of new technology has made possible the local time-resolved determination of the full 3-D velocity gradient tensor[10] at a point in space (Zeff 2003). Knowing the local velocity gradients allows one to calculate the energy dissipation rate ε and mean-square vorticity, $\Omega = \langle\omega^2\rangle/2$, and thereby provide an experimental measure of intense and intermittent dissipation events (see Figure 9).

Both these techniques can be used to obtain large data samples that are statistically converged and have on the order of 10^6 data sets per parameter value. At present, however, the physical length scales accessible to these two techniques are constrained to lie within or close to the dissipation scale ℓ_d. By using holographic methods, one can obtain highly resolved, fully 3-D velocity fields (see Figure 10), which allow the full turbulent inertial range of scales to be investigated (Zhang et al. 1997). For holographic measurements, however, one is limited to a small number of such realizations, and time-resolved measurements are not currently achievable.

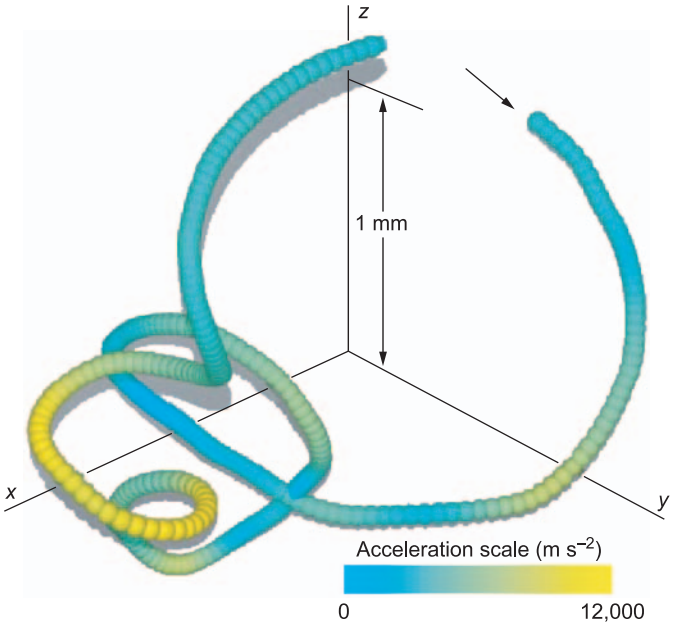

Figure 8. Three-Dimensional Particle Trajectory in a Turbulent Fluid
A high-speed silicon-strip detector was used to record this trajectory of a particle in a turbulent fluid with *Re* = 63,000 (La Porta 2001). The magnitude of the instantaneous acceleration is color-coded. Averaging over many such trajectories allows comparison with the theory of Lagrangian acceleration statistics.
(Modified with permission from *Nature*. This research was performed at Cornell University.)

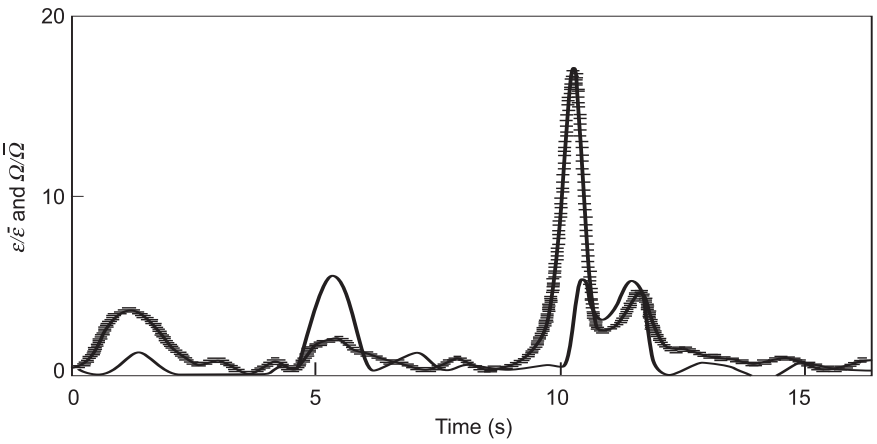

Figure 9. Intermittency of Energy Dissipation and Enstrophy at *Re* = 48,000
Time traces of the local energy dissipation ε (crosses) and enstrophy $\Omega = \langle\omega^2\rangle/2$ (solid curve) illustrate the very intermittent behavior of these dissipation quantities for turbulent flow with *Re* = 48,000 (Zeff 2003). **(Modified with permission from *Nature*. This research was performed at the University of Maryland.)**

Finally, for physical realizations of 2-D flows, full-velocity fields can be measured with high resolution in both space and time (Rivera et al. 2003), and the 2-D velocity gradient tensor can be used to identify topological structures in the flow and correlate them with turbulent cascade mechanisms. The technique used to make these measurements and those represented in Figure 10 is particle-image velocimetry (PIV) or its improved version, particle-tracking velocimetry (PTV). Two digital images, taken

[10] The velocity gradient tensor is a 3×3 matrix consisting of the spatial derivatives of three components of velocity. For example, for the velocity component u_i, the derivatives are $\partial u_i/\partial x_1$, $\partial u_i/\partial x_2$, and $\partial u_i/\partial x_3$.

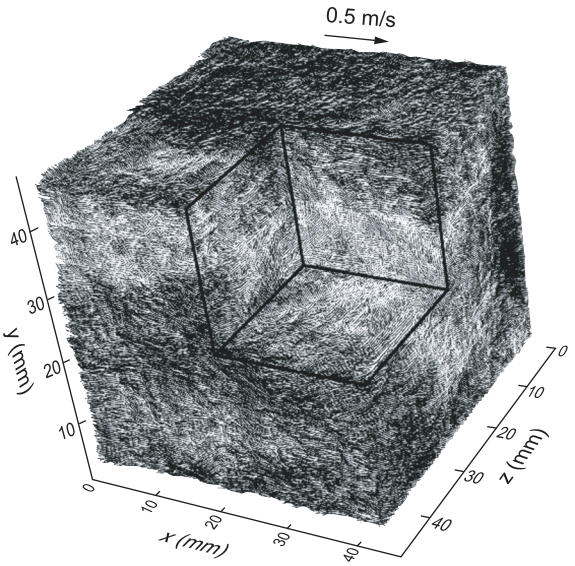

Figure 10. High-Resolution 3-D Turbulent Velocity Fields
These images were obtained using digital holographic particle-imaging velocimetry. (Zhang et al. 1997. Modified with permission from *Experiments in Fluids*.)

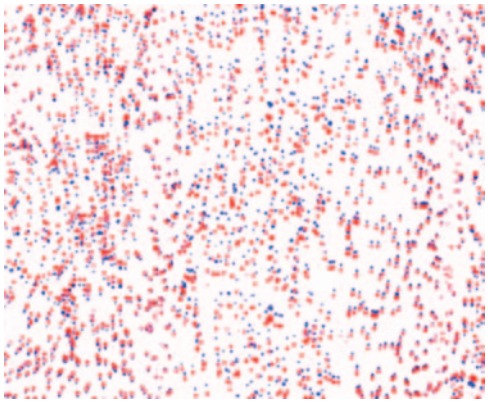

Figure 11. Superimposed Digital Images of a Particle Field
Two digital images of suspended particles taken 0.003 s apart are superimposed. The first exposure is in red; the second, in blue. In PIV, the pattern of particles over a small subregion is correlated between exposures, and an average velocity is computed by the mean displacement δx of the pattern. In PTV, each particle is matched between exposures; as a result, spatial resolution is higher, and there is no spatial averaging. These data allow one to infer the velocity field connecting the two images.

closely spaced in time, track the motion of small particles that seed the flow and move with the fluid. The basic notion is illustrated in Figure 11, where two superimposed digital images of particle fields, separated by $\Delta t = 0.03$ second, are shown. Within small subregions of the domain, patterns of red particles in image 1 can be matched with very similar patterns of blue particles in image 2 by maximizing the pattern correlation. An average velocity vector for the matching patterns is then calculated over the entire box from which a velocity field is obtained, as shown in Figure 12(a). Notice that there are some anomalous vectors caused by bad matching that need to be fixed by some interpolation scheme. PTV, on the other hand, uses a particle-matching algorithm to track individual particles between frames. The resulting vector field is shown in Figure 12(b). The PTV method has higher spatial resolution than PIV but also greater computational-processing demands and more stringent image-quality constraints. From the PTV velocity field, the full vorticity field $\boldsymbol{\omega}$ can be computed as shown in Figure 12(c).

An additional advantage of the PTV approach is that, for high enough temporal resolution, individual particle tracks can be measured over many contiguous frames, and information about Lagrangian particle trajectories can be obtained. Some 2-D particle tracks are shown in Figure 13.

This capability can be combined with new analysis methods for turbulence to produce remarkable new visualization tools for turbulence. Figure 14 shows the full backward and forward time evolution of a marked region of fluid within an identified stable coherent structure (a vortex). These fully resolved measurements in two dimensions will help build intuition for the eventual development of similar capabilities in three dimensions. Further, the physical mechanisms of 2-D turbulence are fascinating in their own right and may be highly relevant to atmospheric or oceanic turbulence.

The Prospects for "Solving" Turbulence

Until recently, the study of turbulence has been hampered by limited experimental and numerical data on the one hand and the extremely intractable form of the Navier-Stokes equation on

(a)

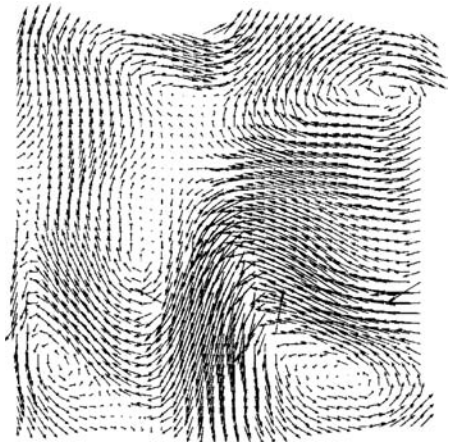

(b)

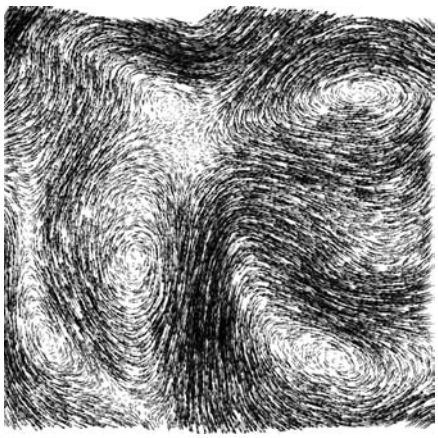

(c)

Figure 12. Two-Dimensional Vector Velocity and Vorticity Fields
The velocities in (a) and (b) were obtained from data similar to those in Figure 11 using PIV and PTV techniques, respectively. The vorticity field in (c) is calculated from the velocity field in (b).

(a)

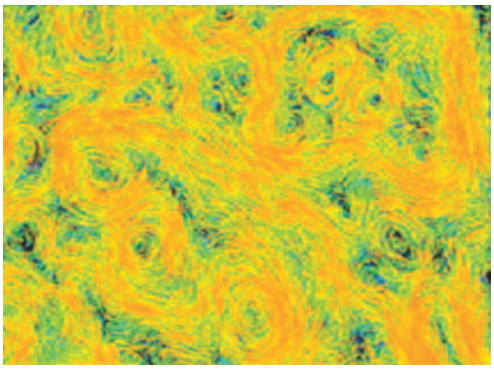

(b)

Figure 13. Individual Lagrangian Particle Tracks for Forced 2-D Turbulence
(a) Approximately 10^4 particles are tracked for short periods. (b) Several individual trajectories are shown for several injection-scale turnover times.

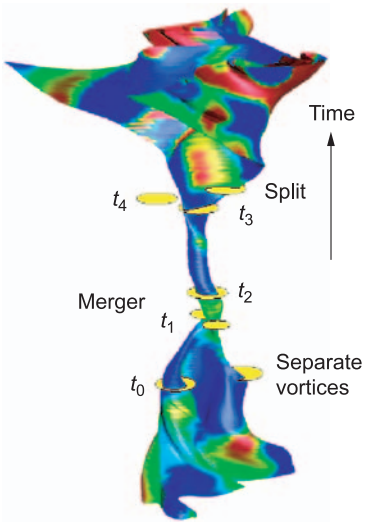

Figure 14. Time Evolution of a Compact Distribution of 10^4 Points in a Coherent Vortex at Time t_2
Vortex merging and splitting happen at times t_1 and t_3, respectively. The color-coding of the surface represents the spatially local energy flux to larger (red) and smaller (blue) spatial scales.
(M. K. Rivera, W. B. Daniel, and R. E. Ecke, to be published in Gallery of Fluid Images, Chaos, 2004.)

the other. Today, the advent of large-scale scientific computation, combined with new capabilities in data acquisition and analysis, enables us to simulate and measure whole velocity fields at high spatial and temporal resolutions. Those data promise to revolutionize the study of fluid turbulence. Further, new emerging ideas in statistical hydrodynamics derived from field theory methods and concepts are providing new theoretical insights into the structure of turbulence (Falkovitch et al. 2001). We will soon have many of the necessary tools to attack the turbulence problem with some hope of solving it from the physics perspective if not with the mathematical rigor or the extremely precise prediction of properties obtained in, say, quantum electrodynamics. Let me explain then what I mean by that solution. In condensed matter physics, for example, the mystery of ordinary superconductivity was solved by the theory of Bardeen, Cooper, and Schrieffer (1957), which described how electron pairing mediated by phonons led to a Bose-Einstein condensation and gave rise to the superconducting state. Despite this solution, there has been no accurate calculation of a superconducting transition temperature for any superconducting material because of complications emerging from material properties. I think that there is hope for understanding the mechanisms of turbulent energy, vorticity, and mass transfer between scales and between points in space. This advance may turn out to be elegant enough and profound enough to be considered a solution to the mystery of turbulence. Nevertheless, because turbulence is probably a whole set of problems rather than a single one, many aspects of turbulence will likely require different approaches. It will certainly be interesting to see how our improved understanding of turbulence contributes to new predictability of one of the oldest and richest areas in physics. ■

Acknowledgments

Three important books on fluid turbulence, McComb (1990), Frisch (1995), and Lesieur (1997), published in the last 20 years have helped provide the basis for this review. I would like to thank Misha Chertkov, Greg Eyink, Susan Kurien, Beth Wingate, Darryl Holm, and Greg Swift for valuable suggestions. I am indebted to my scientific collaborators—Shiyi Chen, Brent Daniel, Greg Eyink, Michael Rivera, and Peter Vorobieff—for many exciting moments in learning about fluid turbulence, and I look forward to more in the future. I would also like to acknowledge the LDRD program at Los Alamos for its strong support of fundamental research in turbulence during the last 5 years

Further Reading

Bardeen, J., L. N. Cooper, and J. R. Schrieffer. 1957. Theory of Superconductivity. *Phys. Rev.* **108** (5): 1175.

Batchelor, G. K. 1952. The Effect of Homogeneous Turbulence on Material Lines and Surfaces. *Proc. R. Soc. London, Ser. A* **213**: 349.

———. 1953. *The Theory of Homogeneous Turbulence*. Cambridge, UK: Cambridge University Press.

———. 1959. Small-Scale Variation of Convected Quantities Like Temperature in Turbulent Fluid. Part 1. General Discussion and the Case of Small Conductivity. *J. Fluid Mech.* **5**: 113.

———. 1969. Computation of the Energy Spectrum in Homogeneous Two-Dimensional Turbulence. *Phys. Fluids* **12**, Supplement II: 233.

Besnard, D., F. H. Harlow, N. L. Johnson, R. Rauenzahn, and J. Wolfe. 1987. Instabilities and Turbulence. *Los Alamos Science* **15**: 145.

Champagne, F. H. 1978. The Fine-Scale Structure of the Turbulent Velocity Field. *J. Fluid Mech.* **86**: 67.

Falkovitch, G., K. Gawedzki, and M. Vergassola. 2001. Particles and Fields in Fluid Turbulence. *Rev. Mod. Phys.* **73**: 913.

Frisch, U. 1995. *Turbulence*: *The Legacy of A. N. Kolmogorov*. Cambridge, UK: Cambridge University Press.

Heisenberg, W. 1948. Zur Statistischen Theorie der Turbulenz. *Z. Phys.* **124**: 628.

Kaneda, Y., T. Ishihara, M. Yokokawa, K. Itakura, and A. Uno. 2003. Energy Dissipation Rate and Energy Spectrum in High Resolution Direct Numerical Simulations of Turbulence in a Periodic Box. *Phys. Fluids* **15**: L21.

Kolmogorov, A. N. 1941a. The Local Structure of Turbulence in Incompressible Viscous Fluid for Very Large Reynolds Number. *Dok. Akad. Nauk. SSSR* **30**: 9

———. 1941b. Decay of Isotropic Turbulence in an Incompressible Viscous Fluid. *Dok. Akad. Nauk. SSSR* **31**: 538.

———. 1941c. Energy Dissipation in Locally Isotropic Turbulence. *Dok. Akad. Nauk. SSSR* **32**: 19.

Kraichnan, R. H. 1959. The Structure of Isotropic Turbulence at Very High Reynolds Numbers. *J. Fluid Mech.* **5**: 497.

———. 1965. Lagrangian-History Closure Approximation for Turbulence. *Phys. Fluids* **8**: 575.

———. 1967. Inertial Ranges in Two-Dimensional Turbulence. *Phys. Fluids **10**:* 1417.

———. 1968. Small-Scale Structure of a Scalar Field Convected by Turbulence. *Phys. Fluids* **11**: 945.

———. 1974. On Kolmogorov's Inertial-Range Theories. *J. Fluid Mech.* **62**: 305.

Lamb, C. 1932. *Address to the British Association for the Advancement of Science. Quoted in Computational Fluid Mechanics and Heat Transfer* by J. C. Tannehill, D. A. Anderson, and R. H. Pletcher. 1984. New York: Hemisphere Publishers.

La Porta, A., G. A. Voth, A. M. Crawford, J. Alexander, and E. Bodenschatz. 2001. Fluid Particle Accelerations in Fully Developed Turbulence. *Nature* **409**: 1017.

Lesieur, M. 1997. *Turbulence in Fluids*. Dordrecht, The Netherlands: Kluwer Academic Publishers.

McComb, W. D. 1990. *The Physics of Fluid Turbulence*. Oxford, UK: Oxford University Press.

Meneveau, C., and J. Katz. 2000. Scale-Invariance and Turbulence Models for Large-Eddy Simulation. *Annu. Rev. Fluid Mech.* **32**: 1.

Obukhov, A. M. 1941. Spectral Energy Distribution in a Turbulent Flow. *Dok. Akad. Nauk. SSSR* **32**: 22.

Onsager, L. 1945. The Distribution of Energy in Turbulence. *Phys. Rev.* **68**: 286.

———. 1949. Statistical Hydrodynamics. *Nuovo Cimento* **6**: 279.

Orszag, S. A., and G. S. Patterson. 1972. In *Statistical Models and Turbulence*, *Lecture Notes in Physics*, Vol. **12**, p. 127. Edited by M. Rosenblatt and C. M. Van Atta. Berlin: Springer-Verlag.

Reynolds, O. 1895. On the Dynamical Theory of Incompressible Viscous Fluids and the Determination of the Criterion. *Philos. Trans. R. Soc. London, Ser. A* **186**: 123.

Richter, J. P. 1970. Plate 20 and Note 389. In *The Notebooks of Leonardo Da Vinci*. New York: Dover Publications.

Richardson, L. F. 1922. *Weather Prediction by Numerical Process*. London: Cambridge University Press.

———. 1926. Atmospheric Diffusion Shown on a Distance-Neighbour Graph. *Proc. R. Soc. London, Ser. A* **110**: 709.

Rivera, M. K., W. B. Daniel, S. Y. Chen, and R. E. Ecke. 2003. Energy and Enstrophy Transfer in Decaying Two-Dimensional Turbulence. *Phys. Rev. Lett.* **90**: 104502.

She, Z. S., S. Y. Chen, G. Doolen, R. H. Kraichnan, and S. A. Orszag. 1993. Reynolds-Number Dependence of Isotropic Navier-Stokes Turbulence. *Phys. Rev. Lett.* **70**: 3251.

Taylor, G. I. 1935. Statistical Theory of Turbulence. *Proc. R. Soc. London, Ser. A* **151**: 421.

———. 1938. The Spectrum of Turbulence. *Proc. R. Soc. London, Ser. A* **164**: 476.

Van Dyke, M. 1982. *An Album of Fluid Motion*. Stanford, CA: Parabolic Press.

von Kármán, T., and L. Howarth. 1938. On the Statistical Theory of Isotropic Turbulence. *Proc. R. Soc. London, Ser. A* **164**: 192.

von Neumann, J. 1963. Recent Theories of Turbulence. In *Collected Works* (1949–1963), Vol. 6, p. 437. Edited by A. H. Taub. Oxford, UK: Pergamon Press.

Zeff, B. W., D. D. Lanterman, R. McAllister, R. Roy, E. J. Kostelich, and D. P. Lathrop. 2003. Measuring Intense Rotation and Dissipation in Turbulent Flows. *Nature* **421**: 146.

Zhang, J., B. Tao, and J. Katz. 1997. Turbulent Flow Measurement in a Square Duct with Hybrid Holographic PIV. *Exp. Fluids* **23**: 373.

For further information, contact Robert Ecke (505) 667-6733 (ecke@lanl.gov).